Molecular Recognition of Modified Adenine Nucleotides by the $P2Y_1$-Receptor. 2. A Computational Approach

Dan T. Major, Efrat Halbfinger, and Bilha Fischer*

Department of Chemistry, Gonda-Goldschmied Center, Bar-Ilan University, Ramat-Gan 52900, Israel

Received April 1, 1999

The molecular recognition of C2- or C8-substituted ATP derivatives by the $P2Y_1$-receptor ($P2Y_1$-R) is analyzed using ab initio quantum mechanical calculations. Parameters that may determine ligand specificity toward $P2Y_1$-R were examined on reduced models and correlated with the biochemical data for the parent compounds. These include tautomerism and protonation energy in the gas and aqueous phases, as well as molecular electrostatic potential (MEP) and dipole moment vector. The calculated electronic parameters cannot explain the inactivity of the C8-substituted ATP derivatives, nor the difference in activity among the C2-substituted ATP analogues. These results indicate that neither tautomerism nor changes in the electronic distribution of the adenine ring play a major role in determining binding specificity of adenine nucleotides to the receptor. It is suggested that the higher potency of the C2-substituted ATP derivatives, compared to ATP, might be due to interaction between the C2 side chain heteroatom and the receptor. Furthermore, the interaction of the C2 alkyl side chain with a hydrophobic pocket at the receptor binding site is suggested. In addition, NMR data in the companion paper indicate that the inactivity of the C8-substituted ATP analogues may be due to steric and conformational, rather than electronic, effects.

Introduction

P2-Receptors (P2-R), which recognize extracellular ATP, represent significant targets for drug development for a variety of pathophysiological conditions.[1] The P2-R superfamily is divided into two major families: G-protein-coupled receptors (P2Y) and ligand-gated ion channels (P2X).[2] Presently, a lack of experimental data on the 3D-structure of these membrane proteins and their mode of ligand binding impedes the comprehension of phenomena such as potency and subtype selectivity. Current approaches used for studying P2-R binding sites include mutational analysis of amino acid residues potentially involved in ATP binding at the P2Y-R[3] and molecular modeling for the construction of models of these receptors and their ligand complexes.[4] A model of the chick $P2Y_1$-R and suggested binding interactions between the protein and ATP have been reported.[4a] An improved model and site-directed mutagenesis studies of the human $P2Y_1$-R have been suggested recently, estimating interactions between ATP or 2-MeS-ATP and the receptor.[4b] In these models, based on rhodopsin as a template, the $P2Y_1$-Rs have a seven-transmembrane helical domain (TM) structure, typical of G-protein-coupled receptors.[4a,b] A model of the human $P2Y_2$-R, based on bacteriorhodopsin, has also been reported.[4c]

The available P2Y-R ligands include ATP analogues modified at the adenine heterocycle, ribose moiety, or triphosphate group[2d,4a,5] or "mini-nucleotide" analogues based on a xanthine alkylphosphate skeleton.[6] In particular, the 2-thioether-ATP derivatives have been shown to be 2−5 orders of magnitude more potent than ATP at the $P2Y_1$-R.[5] Such an enhanced potency may be due to the electron-donating (ED) effect of the thioether group, which changes the charge distribution of the adenine ring, which in turn could optimize interactions with the receptor. Similar reasoning has been used for related systems.[7] However, other effects such as interactions of the thioether side chain with the receptor, through H-bonding or hydrophobic interactions, could also explain the tight fit between 2-thioether-ATP and the $P2Y_1$-R.

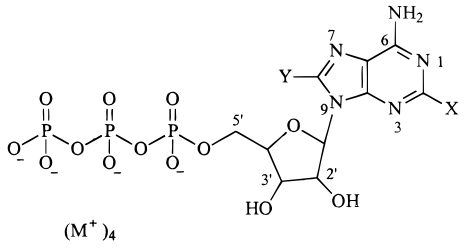

ATP: X = H; Y = H

2-derivatives: X = BuS, BuO, BuHN, Cl; Y = H

8-derivatives: Y = BuS, BuO, BuHN, Br; X = H

Figure 1. ATP derivatives evaluated as $P2Y_1$ agonists.

To investigate the stereoelectronic parameters that determine affinity for the $P2Y_1$-R, a new series of ATP analogues, substituted with ED groups at the C2 or C8 positions of the adenine moiety, was synthesized (Figure 1) and evaluated as $P2Y_1$-R agonists. The synthesis and biochemical and spectral studies are described in part 1.[8] The compounds were tested for their ability to induce $P2Y_1$-R-mediated activation of phospholipase C in turkey erythrocytes and Ca^{2+} response in rat astrocytes. The C2-substituted ATP derivatives increased levels of inositol phosphates and calcium, whereas the C8 substitutions led to ineffective compounds. 2-BuS- and 2-BuHN-ATP were equipotent to 2-MeS-ATP ($K_{0.5}$ 8 nM)[5a] and 3−4 orders of magnitude more potent than

* Address correspondence to: Bilha Fischer, Bar-Ilan University. Tel: 972-3-5318303. Fax: 972-3-5351250. E-mail: bfischer@mail.biu.ac.il.

10.1021/jm9901576 CCC: $18.00
Published on Web 12/09/1999

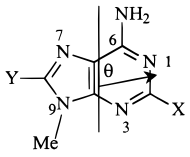

9-Me-adenine: X = H; Y = H

2-derivatives: X = MeS, MeO, MeHN, Cl; Y = H

8-derivatives: Y = MeS, MeO, MeHN, Br; X = H

Figure 2. Reduced models for evaluation of electronic properties. The dipole moment vector is also shown, and its direction is defined by the θ angle.

ATP ($K_{0.5}$ 2800 nM),[5a] while 2-BuO-ATP was the least potent.[8] 2-Cl-ATP was found to be 40 times more potent than ATP and 9 times less potent than 2-MeS-ATP, as was established by measurements of P2Y$_1$-R-promoted phospholipase C activity in turkey erythrocyte membranes.[5a] 8-Br-ATP has been characterized as a poor P2Y$_1$-R agonist, being 17 times less potent than ATP (Figure 1).[5b]

In this paper we report theoretical calculations evaluating the stereoelectronic parameters of the modified purine moiety of ATP that might play a role in the P2Y$_1$-R ligand recognition. For this purpose quantum mechanical (QM) molecular orbital (MO) calculations of properties such as tautomerism, dipole moment vector, probable protonation sites, and molecular electrostatic potential (MEP) have been performed.

Methods

In this study we have investigated various parameters governing ligand recognition by the P2Y$_1$-R. The large size of ATP and the great number of compounds to be screened make QM MO calculations a very demanding task. Furthermore, both the ribose ring and the 5′-phosphate chain introduce conformational flexibility. Therefore, 9-methyl-adenine (9-Me-A) was chosen as a model compound that could effectively mimic the adenine moiety of ATP. The models were further simplified by replacing the thiobutyl chain of the C2 and C8 substituents with a thiomethyl group, assuming that this leaves the electronic properties of the modified purine ring unaffected (Figure 2).

To evaluate the appropriate levels of computation for these model compounds, the ability of several QM MO methods to reproduce the experimental structure and dipole moment of 9-Me-A was investigated. The semiempirical AM1 method[9] and ab initio QM calculations at the Hartree−Fock (HF)[10] level using the 6-31G(d)[11] and 6-311+G(2d,p)[12] basis sets were used. Correlation effects were included using density functional theory (DFT) with the Becke3−Lee−Yang−Parr (B3LYP)[13] functional and the 6-31G(d) and 6-311+G(2d,p) basis sets. The dipole moment in dioxane was also calculated at the ab initio self-consistent reaction field (SCRF) level, using the polarized continuum model (PCM).[14] The PCM calculations were performed with optimized scaling factors and van der Waals radii.[15]

Thereafter, the question of the tautomeric preference of the adenine moiety of ATP and its C2- and C8-substituted analogues was addressed. The molecules investigated were the five tautomers of 9-Me-A and its 2- and 8-substituted derivatives (Figure 3). The energies of the 9-Me-A tautomers and the corresponding 2- and 8-substituted derivatives were calculated at the AM1 (not shown) and HF/6-31G(d) levels with full geometry optimization. Vibrational frequencies were calculated to examine the nature of the stationary points on the potential energy surface. No negative frequencies were found. For the HF/6-31G(d) gas-phase calculations, thermodynamic corrections at a temperature of 310.15 K and pressure of 1 atm were included.

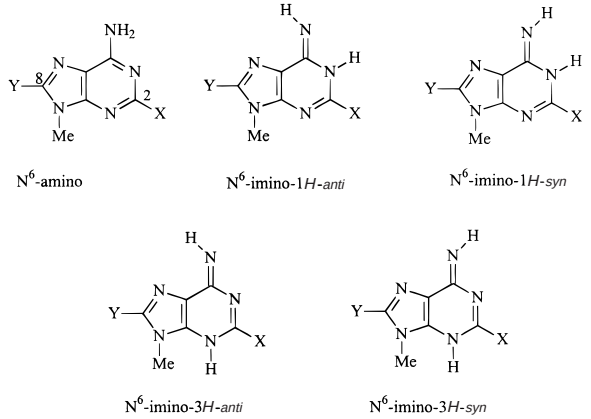

9-Me-adenine: X = H; Y = H

2-derivatives: X = MeS, MeO, MeHN, Cl; Y = H

8-derivatives: Y = MeS, MeO, MeHN, Br; X = H

Figure 3. Tautomers of 9-Me-A and C2- and C8-substituted derivatives.

The free energy of tautomerization in aqueous solution was calculated according to eq 1. In all cases the free energies of tautomerization in the gas phase (ΔG^{gas}(A→B)) were calculated at the HF/6-31G(d) level. Solvent effects were introduced at the semiempirical level, using the AM1-SM2 model.[16] The AM1-SM2 absolute free energies of hydration were calculated relative to the AM1 energy. The corresponding gas-phase optimized geometries were used in all the calculations, since small geometric changes are expected for the rigid molecules investigated[17] and due to convergence problems with the AM1-SM2 model.

$$\Delta G^{aq}(\text{A}\rightarrow\text{B}) = \Delta G^{gas}(\text{A}\rightarrow\text{B}) + \Delta G^{hyd}(\text{B}) - \Delta G^{hyd}(\text{A}) = \Delta G^{gas}(\text{A}\rightarrow\text{B}) + \Delta\Delta G^{hyd}(\text{A}\rightarrow\text{B}) \quad (1)$$

Electronic parameters such as the molecular dipole moment, molecular electrostatic potential (MEP) maps,[18] and protonation free energies in the gas and aqueous phases were calculated for the most stable tautomers. HF/6-31G(d), HF/6-311+G(2d,p), B3LYP/6-31G(d), and B3LYP/6-311+G(2d,p) calculations were performed using the HF/6-31G(d) optimized geometry on the most stable tautomer of 9-Me-A and its 2- and 8-derivatives (Figure 2) and on the protonated species. Only the results of the highest correlated level calculations of dipole moment and protonation energy are presented. Solvent effects on protonation were accounted for using the AM1-SM2 model as before, and the free energy of protonation in solution was calculated according to eq 1. The gas-phase protonation energies (ΔG^{gas}(A→B)) were calculated at the HF/6-31G(d) level. Contributions of the free proton to the free energy of protonation were not included. H-Bonding donor and acceptor patterns were found using the MEP mapped onto an isodensity surface[19] of 0.002 el/au^3 [20] for the AM1 (not shown) and HF/6-31G(d) optimized ligands.

In all cases the ED substituents at C2 or C8 were coplanar with the purine ring. For the dipole moment and MEP calculations, the C2 substituents were in the *anti* conformation which enables H-bonding to N1,[4b] whereas the C8 substituents were in the *syn* conformation (Figure 4).

Finally, the adenine binding pocket of the P2Y$_1$-R in the 2-MeS-ATP:*h*P2Y$_1$-R model complex[4b] was probed for possible interactions of the MeS group with the receptor.

All gas-phase calculations and aqueous-phase PCM calculations were performed using Gaussian 94 and 98,[21] and the AM1 and the HF/6-31G(d) optimized coordinates were imported into PC Spartan 1.0.[22] Single-point calculations were performed to generate the wave functions, using PC Spartan, thus enabling the display of dipole moment vectors and the calculation and display of MEP maps. The 8-Br-9-Me-A HF/6-31G(d) MEP map was not calculated since the PC Spartan

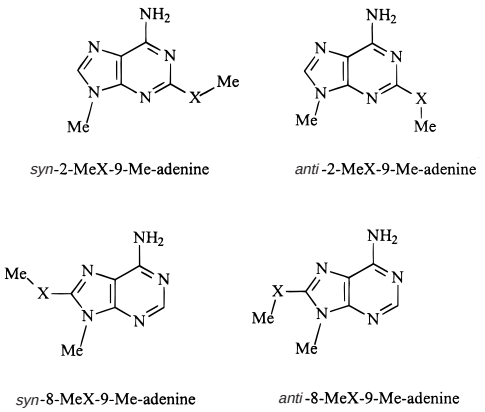

Figure 4. Definition of *syn* and *anti* conformations of the substituent relative to the adenine ring for C2- and C8-substituted 9-Me-A derivatives (X = HN, O, S).

package does not include the 6-31G(d) basis set for Br. AM1-SM2 calculations were performed with PC Spartan 2.7. Calculations with Gaussian 94/98 were performed on an IBM RISC/6000 workstation with the AIX 4 operating system. Analysis of the 2-MeS-ATP:*h*P2Y$_1$-R complex was performed using InsightII 97.2 (Molecular Simulations Inc.) on an SGI O2 R10000 workstation with the IRIX 6.5 operating system.

Results and Discussion

Reduced Model. Several model compounds have been used to mimic the purine and pyrimidine bases of nucleosides and nucleotides or related molecules, to enable QM MO calculations.[17,23] The use of model compounds to calculate tautomerism and other molecular properties is usually necessary since nucleosides and nucleotides are too large for accurate QM MO calculations and the number of tautomers to be screened is often large. Moreover, a model compound representing the modified adenine moiety of ATP may be desirable in order to evaluate the ability of the ligands to interact with the adenine binding pocket of the P2Y$_1$-R. By using a model, one avoids dealing with complexities due to the ribose moiety and the phosphate chain. Thus, a better understanding of the inherent electronic properties of the base, e.g. the charge distribution of the adenine ring as reflected in the dipole moment vector, may be gained.

When choosing a model compound, the ability to reproduce electronic properties of the entire molecule (i.e. ATP) was considered. Replacing the ribose 5′-phosphate moiety with hydrogen or a methyl group seemed to be sound solutions, with the former being simpler. In the gas phase both models give comparable relative tautomeric energies (results not shown). However, in the aqueous phase the results differed considerably (results not shown), since adenine and 9-methylated adenine have different H-bonding patterns, which is reflected in the reaction field created by the homogeneous solvent. Adenine has a greater solvent reaction field than 9-Me-A due to the polar N9-H atom. Indeed, it has been found that methylation of the nucleic acid bases decreases the hydration free energy of the bases by 2−3 kcal/mol.[24] Furthermore, this difference in H-bonding patterns is also reflected in the MEP. Thus, 9-Me-A mimics the purine moiety of ATP better than adenine.

9-CH_2OH-adenine (9-CH_2OH-A) has been found to mimic adenosine with relation to deamination of adenosine by adenosine deaminase.[23b] Therefore, 9-CH_2-OH-A was also considered as a possible model for ATP. However, we found that both the dipole moment vector and the MEP were highly dependent upon the conformation of the hydroxymethylene group. Since there is no straightforward way to constrain the hydroxymethylene group, the model suffers from inconsistency, and no cancellation of errors is expected due to the use of a model compound in a series of 9-CH_2OH-A derivatives. On the other hand, for 9-Me-A it is expected that the errors introduced by using a model compound are similar for the different 2- and 8-substituted derivatives. 9-CH_2OCH_3-A has also been used as a model compound for adenosine in an ab initio investigation into the hydrolysis of adenosine,[23e] but again this model is inconsistent.

Verifying the Calculation Method. Several computational methods were tested for their ability to reproduce the experimental geometry and dipole moment of 9-Me-A. Geometry optimizations were performed at the AM1, HF/6-31G(d), HF/6-311+G(2d,p), B3LYP/6-31G(d), and B3LYP/6-311+G(2d,p) levels. Our DFT calculations are comparable to previous results of Holmén and Broo.[25] No restrictions were imposed on the molecule, as it has been found both in crystallographic[26a,b] and spectroscopic[26c] studies and in theoretical works[27] that nucleic acid bases are not completely planar. Two energy minima and one transition state were found at the HF and B3LYP levels using the 6-31G(d) and 6-311+G(2d,p) basis sets. The two energy minima correspond to the two possible out-of-plane conformations of the N^6 amino group.[25] However, using AM1 the in-plane N^6 conformation gave a local minimum. The calculated geometries were compared with the geometry determined using neutron diffraction measurements[28a] and are shown in Table 1 together with the average bond length and bond angle deviations from the experimental structure. The HF bond lengths are too short by about 0.014 and 0.017 Å, with an increasing deviation as the basis set increases from 6-31G(d) to 6-311+G-(2d,p). This is corrected when electron correlation is included, and the absolute deviation is 0.007 and 0.008 Å when using the B3LYP functional with 6-31G(d) and 6-311+G(2d,p) basis functions, respectively. The results obtained using the B3LYP functional are comparable to results found using second-order Møller−Plesset perturbation theory (MP2),[29] but with a considerably reduced computational effort. Both HF and DFT bond angles are good, with absolute deviations of 1.0°. An extended basis set in the HF or DFT B3LYP framework does not improve the calculated geometry, and HF/6-311+G(2d,p) actually gives less satisfactory bond distances than HF/6-31G(d).

The calculated dipole moments of 9-Me-A in the gas phase and in dioxane compared to the experimental value[30] are shown in Table 2. The dipole moment is sensitive both to the level of theory and to the size of the basis set. The calculated dipole moments in the gas phase are lower than the experimental value of 3.25 D.[31] AM1 gives the least satisfactory result with a deviation of 0.95 D. HF/6-31G(d) resulted in a dipole moment of 2.72 D, while using HF/6-311+G(2d,p) yielded a dipole moment of 2.80 D, which was the closest to the experimental. There was also an improvement when increas-

Table 1. Comparison of the Calculated Geometry[a] of 9-Me-A at Different Levels of Theory and the Experimental Neutron Diffraction Geometry[b]

	AM1	HF/6-31G(d)	HF/6-311+G(2d,p)	B3LYP/6-31G(d)	B3LYP/6-311+G(2d,p)	expt[b]
N1−C2	1.360	1.328	1.326	1.344	1.340	1.344
C2−N3	1.353	1.313	1.310	1.337	1.332	1.331
N3−C4	1.368	1.329	1.327	1.340	1.336	1.344
C4−C5	1.459	1.377	1.373	1.399	1.395	1.396
C5−C6	1.436	1.400	1.395	1.410	1.405	1.416
C6−N1	1.376	1.327	1.323	1.345	1.340	1.355
C5−C7	1.402	1.381	1.380	1.384	1.382	1.388
N7−C8	1.341	1.282	1.279	1.312	1.308	1.323
C8−N9	1.417	1.370	1.366	1.381	1.377	1.368
N9−C4	1.402	1.362	1.360	1.379	1.376	1.372
C6−N10	1.369	1.346	1.347	1.359	1.356	1.340
N9−C15	1.424	1.447	1.445	1.452	1.452	1.455
N1−C2−N3	130.3	128.7	128.5	128.9	128.4	128.8
C2−N3−C4	112.5	111.6	111.8	111.1	111.6	110.7
N3−C4−C5	123.7	126.4	126.3	126.9	126.5	127.4
C4−C5−C6	117.1	116.1	116.2	115.8	116.1	116.4
C5−C6−N1	118.8	118.6	118.6	118.9	118.6	117.2
C6−N1−C2	117.5	118.6	118.7	118.3	118.7	119.5
N3−C4−N9	130.9	128.2	128.1	127.9	128.2	126.7
C5−N7−C8	105.1	103.8	103.9	103.6	103.9	103.8
N7−C8−N9	113.7	114.4	114.3	114.2	114.0	113.9
C8−N9−C4	106.0	105.6	105.6	105.8	105.8	106.1
N9−C4−C5	105.3	105.4	105.6	105.1	105.3	105.9
C4−C5−N7	110.0	110.8	110.6	111.3	111.0	110.4
C6−C5−N7	132.9	133.2	133.2	132.9	132.9	133.2
N10−C6−C5	120.2	122.4	122.5	122.3	122.4	124.3
N10−C6−N1	121.0	118.9	118.9	118.8	118.9	118.5
C8−N9−C15	127.0	128.0	127.8	128.1	127.8	128.3
C15−N9−C4	126.9	126.4	126.7	126.2	126.3	125.6
N1−C6−N10−H13	−1.0	11.8	13.8	13.3	11.6	5.3
C5−C6−N10−H14	1.0	−12.6	−14.4	−14.3	−12.0	−13.1
C2−N1−C6−N10	−179.8	178.5	178.2	178.1	178.3	179.0
$\langle\Delta x\rangle$[c]	−0.023	0.014	0.017	−0.001	0.003	
$\langle\Delta x_{abs}\rangle$[d]	0.028	0.016	0.018	0.007	0.008	
$\langle\Delta\theta\rangle$[e]	−0.1	0.0	0.0	0.0	0.0	
$\langle\Delta\theta_{abs}\rangle$[f]	2.3	1.0	1.0	1.0	1.0	

[a] Bond lengths are in Ångström, and bond and dihedral angles are in degrees. [b] Ref 28a. [c] Mean bond length deviation. [d] Mean absolute bond length deviation. [e] Mean bond angle deviation. [f] Mean absolute bond angle deviation.

Table 2. Calculated Dipole Moments of 9-Me-A at Various Computational Levels, Compared with the Experimental Value

method[a]	dipole moment[b] (D)	expt[c] (D)
A	2.30	3.25 ± 0.2 (dioxane)
B	2.72	
C	2.80	
D	2.57	
E	2.70	
F	3.10	

[a] Method A, AM1//AM1; B, HF/6-31G(d)//HF/6-31G(d); C, HF/6-311+G(2d,p)//HF/6-31G(d); D, B3LYP/6-31G(d)//B3LYP/6-31G(d); E, B3LYP/6-311+G(2d,p)//B3LYP/6-31G(d); F, B−PCM. [b] The dipole moment vector angle was defined as the clockwise angle between the axis from C4 to C5 and the dipole moment vector (Figure 2). [c] Refs 30 and 31.

ing the B3LYP basis set from 6-31G(d) to 6-311+G(2d,p) with values of 2.57 and 2.70 D, respectively. This shows that a wider basis set is needed to achieve a better description of the charge distribution. In this context, it is worth noting that 9-Me-A in the N^6 out-of-plane conformation has a greater dipole moment compared to the in-plane conformation, with differences of up to 0.2 D. Thus, accounting for the nonplanarity of the N^6 amino group improves the calculated dipole moment. Furthermore, inclusion of the solvent effects of dioxane on the dipole moment improves the results compared to experiment, with a value of 3.10 D using HF/6-31G(d). Therefore, it is necessary to account for solvation of the solute, even by a nonpolar solvent, to accurately reproduce the experimental dipole moment value.

Tautomerism. 9-Me-A has several possible tautomeric structures (Figure 3). Each tautomer has a specific H-bonding donor and acceptor pattern, which may determine molecular recognition. Moreover, from this pattern the nature of the amino acid residues participating in the receptor−ligand complex may be deduced. Therefore, the possible effects of ED or electron-withdrawing (EW) substituents at the C2 or C8 positions of the adenine ring on the relative stability of the tautomers were considered. The most stable tautomer in the gas or aqueous phases is not necessarily the one preferred by the receptor. However, a considerable large energy difference between the tautomers does indicate which one will be dominant at the receptor site. Five tautomers of each derivative, one amino and four imino species (Figure 3), were considered in the gas and aqueous phases. It has been determined experimentally that for adenosine, the amino tautomer is the most dominant, with less than 0.001% population estimated for the imino tautomer in a variety of solvents with different dielectric constants.[32a] It has also been found that the 6-amino-9H tautomer of adenine is the most stable in the gas phase,[26c] although the metal-stabilized imino tautomer of 9-Me-A has been observed.[32b] Furthermore, semiempirical[33] and ab initio[34] QM MO

Table 3. Differences in Free Energy in the Gas Phase Relative to the Most Stable Tautomer for Tautomers of 9-Me-A and Its 2- and 8-Substituted Derivatives at 310.15 K and 1 atm Using HF/6-31G(d)[a]

	ΔG_{gas} (kcal/mol)								
tautomer[b]	2-H	2-MeS	2-MeO	2-MeHN	2-Cl	8-MeS	8-MeO	8-MeHN	8-Br
6-imino-*anti*-1*H*-purine	15.2	16.1	12.8	17.3	18.1	15.4	16.3	16.6	15.5
6-imino-*syn*-1*H*-purine	22.6	23.0	19.8	25.1	25.2	22.1	23.0	23.6	22.5
6-imino-*anti*-3*H*-purine	35.1	33.9	30.8	37.2	36.9	34.5	36.0	36.5	35.4
6-imino-*syn*-3*H*-purine	34.2	34.0	30.7	37.5	36.2	35.5	34.8	37.1	34.4

[a] HF/6-31G(d)//HF/6-31G(d). [b] Definition of the tautomers is given in Figure 3.

Table 4. Differences in Free Energy in the Aqueous Phase Relative to the Most Stable Tautomer for Tautomers of 9-Me-A and Its 2- and 8-Substituted Derivatives Using AM1-SM2[a]

	ΔG_{aq} (kcal/mol)								
tautomer[b]	2-H	2-MeS	2-MeO	2-MeHN	2-Cl	8-MeS	8-MeO	8-MeHN	8-Br
6-imino-*anti*-1*H*-purine	13.8	13.6	14.3	16.5	19.2	14.1	14.5	14.9	13.3
6-imino-*syn*-1*H*-purine	22.0	21.8	21.6	25.0	26.8	20.0	23.4	23.6	21.5
6-imino-*anti*-3*H*-purine	30.7	29.6	30.5	35.2	35.9	35.0	41.9	35.4	33.0
6-imino-*syn*-3*H*-purine	31.9	30.4	30.9	35.1	38.1	32.2	33.3	34.9	32.5

[a] The aqueous-phase tautomerism was calculated according to eq 1. [b] Definition of the tautomers is given in Figure 3.

calculations on adenine and 9-Me-A all indicate that the amino tautomer is by far the most stable one.

Gas-Phase Tautomeric Calculations. Free energy calculations of the tautomerism of 9-Me-A in the gas phase showed that the differences in energy between the amino and imino tautomers (Figure 3) were 15.3 kcal/mol or more in favor of the amino tautomer (Table 3). The order of stability was 6-amino-purine > 6-imino-*anti*-1*H*-purine > 6-imino-*syn*-1*H*-purine > 6-imino-*anti*-3*H*-purine, 6-imino-*syn*-3*H*-purine. The pyrimidine ring in 6-amino-purine is aromatic; this is probably the main reason for it being the most stable tautomer.[33a] When comparing the imino tautomers, it seems that the N1-H purines have more favorable conjugation than the N3-H purines and they are more stable than the latter by about 10−20 kcal/mol. The difference between *anti*-N1-*H* and *syn*-N1-*H* is 7.2 kcal/mol and is probably due to hydrogen−hydrogen repulsion between the N^6 and N1 hydrogens in the *syn* tautomer. This explanation is further supported by the similar energies of the two N3-H purine tautomers.

Next, the effect of C2 and C8 ring substitutions (Figure 3) on the relative stability of the 9-Me-A tautomers was explored. In all our free energy calculations in the gas phase, the difference in energy between the amino and imino tautomers of the 9-Me-A analogues (Figure 3) was at least 12.6 kcal/mol in favor of the amino tautomer. Moreover, the relative stability of the tautomers of the 9-Me-A analogues was similar to the order of stability obtained for 9-Me-A (Table 3). The 2-MeO substitution stabilizes the imino relative to the amino tautomer by about 3 kcal/mol compared to the 9-Me-A tautomers. This may be explained by the favorable conjugation between the methoxy oxygen's perpendicular lone pair and the pyrimidine ring, which stabilizes the nonaromatic imino relative to the amino species. This effect is absent in the 2-MeHN and 2-MeS derivatives. The 2-MeHN-6-imino tautomers are destabilized relative to the amino by about 2−4 kcal/mol when compared with the parent compound. This might be due to repulsion between the hydrogens at the N1 or N3 positions and the 2-MeHN group. The 2-MeS-9-Me-A tautomers show almost the same relative energies between the amino and imino species as are observed for the 9-Me-A tautomers. This is probably due to the ineffective overlap between the carbon 2p and sulfur 3p atomic orbitals. The 2-Cl substitution destabilized the 6-imino tautomers relative to the amino by about 2−6 kcal/mol when compared with 9-Me-A, probably due to its EW nature. All the imidazole ring substitutions had little effect on the relative tautomeric energies when compared with the parent compounds.

Aqueous-Phase Tautomeric Calculations. The aqueous solvent effects on tautomerism of 9-Me-A and its 2- and 8-substituted analogues were examined by means of the AM1-SM2 model. Inspection of the results in Table 4 shows that the tautomeric preference in the gas phase is not drastically altered upon transfer to solution. The difference between the amino and imino tautomers is at least 13.3 kcal/mol. Thus the amino tautomer is clearly the most stable species in an aqueous solution as well.

In conclusion, the tautomeric preference of 9-Me-A is not significantly changed upon substitution with ED or EW substituents at either the C2 or C8 position. Similar results were obtained in a study on 5-bromo-uridine.[35] Thus, we may assume that the amino tautomer is the dominant and biologically active one and that the H-bonding pattern is the same for the adenine moiety in ATP and in the 2- and 8-modified adenine nucleotides.

Electronic Properties. Knowledge of the inherent electronic properties of the adenine moiety of ATP and its C2- and C8-substituted derivatives is important for rationalizing their complementarity with the $P2Y_1$-R binding site. A priori, the relative affinities reported (2-MeS-ATP > 2-Cl-ATP > ATP) imply that electronic effects alone do not explain the difference in $P2Y_1$-R activity. However, to explore to what degree the electronic changes of the adenine ring due to ED or EW substituents at the C2 or C8 positions govern ligand binding, the dipole moment, MEP, and protonation energies of the corresponding models were examined. Furthermore, the possibility that the substituent itself is responsible for the enhanced biological activity, through H-bonding or hydrophobic interactions with the receptor, was also investigated.

Dipole Moment. The dipole moment vector provides information about the charge distribution in a molecule and may thus account for electronic effects involved in

Table 5. Dipole Moment Vectors of 9-Me-A and Its 2- and 8-Substituted Derivatives in the Gas Phase Calculated at the B3LYP/6-311+G(2d,p) Level[a]

derivative[b]	dipole moment (D)	angle[c] (deg)
9-Me-A	2.70	81.7
2-MeO-9-Me-A	3.30	57.0
2-MeS-9-Me-A	3.59	65.6
2-MeHN-9-Me-A	1.66	18.5
2-Cl-9-Me-A	4.24	100.0
8-MeO-9-Me-A	3.86	104.9
8-MeS-9-Me-A	3.26	112.2
8-MeHN-9-Me-A	4.64	87.3
8-Br-9-Me-A	1.41	80.9

[a] Method: B3LYP/6-311+G(2d,p)//B3LYP/6-31G(d). [b] Structures of the compounds are given in Figure 2. [c] The dipole moment vector angle was defined as the clockwise angle between the axis from C4 to C5 and the dipole moment vector (Figure 2).

molecular recognition. The dipole moment vector of 9-Me-A points from the pyrimidine ring to the imidazole ring, i.e. the pyrimidine ring has greater electron density (Figure 2). This has been shown to be mainly due to the π-component of the electron population in the case of adenine.[34] The direction of the dipole moment vector was defined as the clockwise angle between the axis from C4 to C5 and the dipole moment vector (θ angle, Figure 2). The calculated dipole moment vectors are given in Table 5. It was expected that the 8-ED groups and 2-Cl would increase the dipole moment vector size and that the 2-ED groups and 8-Br would lead to a decreased dipole moment when compared to 9-Me-A, based upon traditional resonance structures and the electronegativity of the halides. This estimation was found to be true for the 2-Cl- and 8-Br-substituted derivatives and for the 2- and 8-MeHN-substituted compounds, but not in the case of the MeS and MeO derivatives. A reasonable explanation for these exceptions might be the in-plane lone pair of the sulfur and oxygen groups at the C2 or C8 positions of the adenine ring. The localized in-plane σ-lone pair probably has a greater effect on the dipole moment vector than the conjugated perpendicular π-lone pair.

There is no clear correlation between the dipole moment vectors and the biological activities of the ligands at the P2Y$_1$-R.[5a,8] 2-Cl-ATP, 2-BuS-ATP, and 2-BuHN-ATP show increased activity compared to ATP. However, there is no apparent common substituent effect on the dipole moment vector. Therefore, the dipole moment vector of the adenine moiety cannot explain the great increase in potency of the C2-substituted ATP ligands. Furthermore, the inactivity of the C8-substituted compounds cannot be explained in terms of the dipole moment vector.

Moreover, the size and direction of the dipole moment vector was found to be highly dependent on the substituent conformation in the case of the ether and thioether analogues, due to the in-plane lone pair of the substituent heteroatom. This leads to ambiguity when correlating between the ligand dipole moment vectors and the potencies toward the P2Y$_1$-R. Consequently, the dipole moment vector of the model compounds might not be a suitable parameter to describe the charge distribution of the ligand, especially in cases where the active conformation is unknown.

N^6 Conformation and MEP. Since the N^6 amino group is thought to play a central role in recognition of ATP and its analogues by the P2Y$_1$-R,[3b,4a,b] it was of interest to investigate how the change in charge distribution due to the C2 or C8 substitutions influences its nature. It was found that the 2- and 8-ED substituents lead to a larger out-of-plane deformation, while the EW substituents increase the sp^2 character of the N^6 amino group. Furthermore, the 8-ED groups had a greater effect on the N^6 conformation than the 2-ED groups, as the conjugation between the C8 and C6 positions is stronger than that between the C2 and C6 positions. The 2- and 8-MeHN and MeO substituents had greater influence than the MeS substituent. The 2-Cl substitution caused significantly larger changes in the N^6 conformation than did the 8-Br counterpart. This may be explained by both the differences in electronegativity and the proximity to the C6 position.

Table 6. MEP Values at the 0.002 el/au^3 Isosurface (kcal/mol) in the Vicinity of Selected Hydrogen Bond Donors and Acceptors of 9-Me-A and Its 2- and 8-Substituted Derivatives Using HF/6-31G(d)[a,b]

	N1	N3	N7	N^6	H13	H14
9-Me-A	−45.40	−43.14	−42.37	−25.98	54.03	52.83
2-MeO-9-Me-A	−55.61	−33.79	−43.40	−23.15	52.18	53.69
2-MeS-9-Me-A	−46.05	−32.41	−41.19	−21.73	53.90	54.27
2-MeHN-9-Me-A	−40.27	−41.80	−46.51	−28.21	52.22	49.21
2-Cl-9-Me-A	−44.16	−41.89	−38.04	−13.47	59.03	59.67
8-MeO-9-Me-A	−46.72	−44.67	−35.67	−31.15	51.66	50.79
8-MeS-9-Me-A	−45.03	−40.04	−32.36	−26.32	53.88	53.90
8-MeHN-9-Me-A	−48.35	−41.98	−42.43	−33.73	49.80	48.10

[a] HF/6-31G(d)//HF/6-31G(d). [b] The 6-31G(d) basis set is not included for Br in PC Spartan 1.0; thus no results are shown.

The 0.002 el/au^3 MEP map of 9-Me-A shows three clear minimum values, $V(r)_{min}$, in the in-plane lone pair regions of N1, N3, and N7, which is in accordance with experimental findings,[28b] indicating that these heteroatoms are H-bond acceptors (Table 6). Similar results have been found in theoretical works on adenine.[36] In the N^6 lone pair region a much smaller minimum was found. The two N^6 hydrogens showed clear maxima, $V(r)_{max}$, which suggests that they may participate in hydrogen bonds as donors. This strengthens previous modeling studies, which predict interaction between an N^6 hydrogen and the carbonyl of Gln307.[4b] A report on mono- and dimethylation of the N^6 position in ATP which significantly reduces potencies of P2Y$_1$-R ligands further supports the role of N^6 hydrogens in binding to the P2Y$_1$-R.[5a,b]

2-MeO-9-Me-A had a significantly greater minimum in the MEP near N1 relative to 9-Me-A, as a result of the increased electron density at the N1 position and as a result of the neighboring oxygen (Figure 5). This oxygen may also function as an H-bond acceptor, through its in-plane lone pair. 2-MeS-9-Me-A had a $V(r)_{min}$ value in the vicinity of N1 similar to that of 9-Me-A, since sulfur is less electronegative than oxygen. The sulfur atom had a minimum in $V(r)$ perpendicular to the purine plane (Figure 5). Recent theoretical and crystallographic studies comparing oxygen and sulfur as H-bond acceptors show that oxygen donates its n_σ lone pair, whereas sulfur donates its n_π lone pair.[37] For the 2-MeHN derivative there was an increase in $V(r)$ in the vicinity of N1. This is a result of the amine hydrogen that partly blocks the N1 position. The 2-MeHN group may H-bond through its hydrogen, which shows a clear maximum in the MEP (Figure 5). The 2-Cl

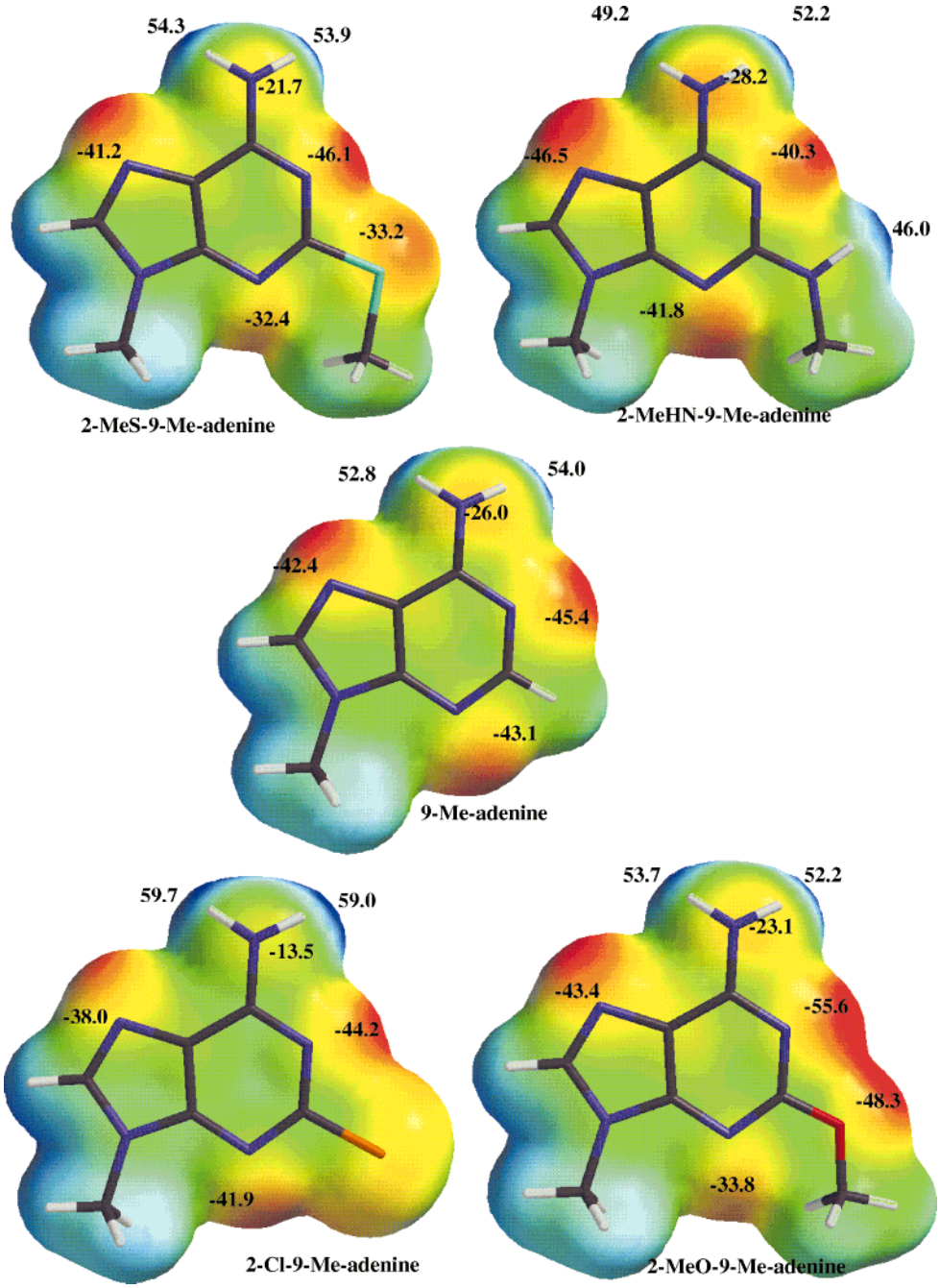

Figure 5. MEP mapped onto the 0.002 el/au^3 isodensity surface of 9-Me-A and the 2-substituted 9-Me-A derivatives.

derivative had a similar $V(r)_{min}$ value near N1 to that of 9-Me-A (Figure 5). The 8-MeHN and 8-MeO groups led to lower N1 $V(r)_{min}$ values, although in general the C8-substitutions had less impact on the N1 position.

The 8-ED group partly blocked the N7 position, and thus the $V(r)_{min}$ value was more positive relative to 9-Me-A. The 2-MeHN and 2-MeO substitutions slightly decreased the $V(r)_{min}$ value at N7, thus increasing their ability to participate in H-bonding.

Substituting the adenine ring with an ED group at the C8 position had a significantly larger influence on the $V(r)_{min}$ value of N^6 than at the C2 position, decreasing the value of the MEP in the lone pair region of N^6. 2-Cl-9-Me-A showed a large increase in the $V(r)_{max}$ value of the two N^6 hydrogens, as a result of the increased polarity of the N^6-H bonds.

We may conclude that there is no clear correlation between the MEP values in the vicinity of the N1, N3, N7, and N^6-H positions and the biochemical data that explains the inactivity of the 8-substituted compounds versus the activity of the 2-substituted derivatives. Furthermore, the difference in activity of the series of 2-substituted compounds is also not explained by the MEP of the adenine moiety. However, the 2-ED substituents each have the ability to H-bond to the receptor. The 2-MeS and 2-MeO groups both function as H-bond acceptors, although they differ in heteroatom size and directionality in H-bonding, while the 2-MeHN group may function both as an acceptor and as a donor. On the other hand, the N^6 hydrogens of the 2-Cl derivative have increased H-bond donor character, and this may explain its increased activity.

Table 7. Protonation Free Energy in the Gas Phase of 9-Me-A and Its 2- and 8-Substituted Derivatives at 310.15 K and 1 atm using B3LYP/6-311+G(2d,p)[a]

	ΔG_{gas} (kcal/mol)								
	2-H	2-MeS	2-MeO	2-MeHN	2-Cl	8-MeS	8-MeO	8-MeHN	8-Br
N1-H-9-Me-A	−233.2	−233.6	−239.9	−239.2	−226.0	−232.9	−234.7	−238.2	−228.3
N3-H-9-Me-A	−230.6	−233.2	−238.2	−237.0	−223.7	−230.8	−232.3	−234.4	−225.1
N7-H-9-Me-A	−226.1	−225.7	−227.8	−233.2	−221.0	−225.7	−226.3	−236.5	−208.2

[a] B3LYP/6-311+G(2d,p)//B3LYP/6-31G(d).

Table 8. Protonation Free Energy in Aqueous Solution of 9-Me-A and Its 2- and 8-substituted Derivatives Using AM1-SM2[a]

	ΔG_{aq} (kcal/mol)								
	2-H	2-MeS	2-MeO	2-MeHN	2-Cl	8-MeS	8-MeO	8-MeHN	8-Br
N1-H-9-Me-A	−277.6	−276.7	−277.3	−275.9	−267.4	−273.2	−278.0	−279.3	−273.7
N3-H-9-Me-A	−272.0	−272.1	−271.8	−271.2	−261.7	−268.5	−272.1	−272.4	−266.6
N7-H-9-Me-A	−272.8	−269.5	−273.1	−275.1	−269.6	−265.9	−262.8	−272.7	−248.6

[a] ΔG_{aq} was calculated according to eq 1.

Protonation Energy. The presence of amino acid side chains bearing acidic protons in the neighborhood of the P2Y$_1$-R adenine binding pocket[4b] necessitates the investigation of possible protonation sites. In the *h*P2Y$_1$-R model proposed by Moro et al.,[4b] the possibility of ionic interaction between N7 of the adenine ring in ATP and Arg310 is mentioned. It is well-established that the adenine ring nitrogens rather than the N^6 amino group are protonated.[38a] The order of protonation in aqueous solution of the purine moiety of adenosine 5′-diphosphate found experimentally is N1 > N7, N3, whereas a second protonation occurs at N7.[38a]

Gas-Phase Protonation. For 9-Me-A, the most favorable calculated protonation site is N1 (Table 7), while protonation at N3 is less favorable by 2.6 kcal/mol and protonation at N7 is 7.1 kcal/mol less favorable. These results are in agreement with previous theoretical studies of adenine[39a] and 9-Me-A.[39b] The order of protonation is not altered upon C2 or C8 substitution. However, the ED substituents stabilize the protonated species, whereas the EW substituents destabilize the protonated species.

Aqueous-Phase Protonation. In all cases, the free energy of protonation was greater in aqueous solution than in the gas phase, as might be expected (Table 8). The relative order of proton affinity is somewhat altered upon transfer to solution. For 9-Me-A and the 2-substituted analogues, the proton affinity of N1 and N7 is increased relative to N3. This may be a result of decreased repulsion between the N1 or N7 proton and the N^6 hydrogen, due to the presence of the solvent. For the 8-substituted derivatives, the relative aqueous-phase proton affinities are similar to that in the gas phase.

Again, there is no clear correlation between the basicity of the purine ring nitrogens and the affinity of the ligands for the P2Y$_1$-R, and the conclusions are similar to those previously mentioned.

Conclusion

The origin of the high potency of several modified ATP derivatives (Figure 1) regarding P2Y$_1$-R was explored in these companion papers by theoretical calculations and experimental methods.[8] 9-Me-A and its C2- and C8-substituted derivatives were used as models for the above-mentioned set of P2Y$_1$-R ligands in calculations evaluating various electronic properties of the purine ring system (Figure 2).

The relative stability of the tautomers of 9-Me-A and its C2- and C8-substituted derivatives (Figure 3) was established by QM MO calculations. The N^6 amino tautomer was found to be the dominant one in both the gas and aqueous phases for all the derivatives of 9-Me-A investigated. This suggests that the amino tautomer is also that which binds to the P2Y$_1$-R site. Thus we may conclude that the H-bonding pattern required for binding to the receptor is the same for all the ligands.

In the *h*P2Y$_1$-R model proposed by Moro et al.,[4b] the adenine moiety of ATP binds to the receptor through H-bonds involving N1, N^6-H, and N7. The P2Y$_1$-R agonist 2-MeS-ATP, on the other hand, is suggested as binding only through N^6-H. The ligand is moved further away from Ser314 due to the 2-MeS group, thus weakening the N1 H-bond with Ser314. However, the phosphate group binds more favorably to the binding site than ATP, due to enhanced interactions with positively charged amino acids.[4b] However, in our opinion, further interactions between 2-MeS-ATP and the receptor are possible, such as H-bonding of the sulfur atom with an H-donor in the binding site. In the model proposed by Moro et al., the sulfur atom is 3.66 Å from the Ser314 oxygen,[4b] which is within H-bonding distance for sulfur compounds. Indeed, in a recent high-level ab initio study of H-bonding interactions in proteins, the equilibrium distance for an H-bond between Ser and Met is 3.64 Å.[40] The greater size of the sulfur atom and its n_π lone pair donor character may explain the increased activity of 2-BuS-ATP over that of 2-BuO-ATP. Furthermore, the substituent's methyl group is surrounded by numerous hydrophobic amino acids, according to Moro's model (Table 9).[4b] Such a hydrophobic pocket may explain the fact that increasing the length of the thioether side chain in 2-RS-ATP ligands enhances the affinity toward the P2Y$_1$-R.[5a] Thus, we hypothesize that both the substituent heteroatoms and the alkyl groups play important roles in the recognition of the novel 2-substituted ATP derivatives by the P2Y$_1$-R, rather than changes in the charge distribution of the purine ring.

The above hypothesis cannot explain the increased activity of 2-Cl-ATP.[5a] However, like 2-MeS-ATP, this compound might be moved into a more favorable position, and the large Cl atom may give rise to a tighter

Table 9. Amino Acid Residues of the hP2Y$_1$-R within Distance of 10 Å of the Methyl Group of 2-MeS-ATP[a]

	aa residues	no. of aa residues
Ala	313	1
Arg	310	1
Asn	316	1
Asp	320	1
Cys	318	1
Gln	307	1
Gly	65, 137, 311	3
His	132	1
Ile	108, 139	2
Leu	104, 107, 134, 140, 142, 312, 315	7
Phe	62, 66, 131, 141, 269, 276	6
Pro	321	1
Ser	138, 272, 314, 317	4
Thr	143, 309	2
Tyr	58, 100, 111, 135, 136, 273	6
Val	133, 319	2

[a] Based on the model of the hP2Y$_1$-R:2-MeS-ATP complex in ref 4b.

fit between ligand and receptor. Furthermore, the increased H-bonding donor character of the N^6 hydrogens of the 2-Cl derivative, as seen by the MEP, may explain enhanced interactions with the receptor.

The reason for the inactivity of the 8-substituted ATP analogues may be steric rather than electronic, as is discussed in the companion article.[8] It is known that 8-Br-adenosine prefers the *syn* conformation around the glycosidic bond.[38b] Furthermore, our NOESY experiments for the 2- and 8-BuS-, BuO-, and BuHN-adenosine prove that the C2-substituted analogues prefer the *anti* conformation while the 8-BuS and 8-BuO derivatives prefer the *syn* conformation due to steric hindrance.[8] Examination of various protein:ATP complexes available in the PDB indicated that ATP binds in the *anti* conformation. The preference of the C8-substituted ATP derivatives for the *syn* conformation might explain their inactivity. Another possibility is that the C8 substituent is not well-accommodated for by the receptor, due to steric hindrance.

Acknowledgment. This work was supported in part by German−Israeli Foundation (GIF) Grant No. I-513-210.09/96 and the Marcus Center for Pharmaceutical and Medicinal Chemistry. We thank Dr. Stefano Moro for providing us with the PDB files of the hP2Y$_1$-R:ligand complexes.

References

(1) (a) Stone, T. W.; Simmonds, H. A. *Purines: Basic and Clinical Aspects*; Kluwer Academic Publishers: MA, 1991; pp 1−245. (b) Spedding, M.; Williams, M. Development in purine and pyrimidine receptors based therapeutics. *Drug Dev. Res.* **1996**, *39*, 436−441. (c) Abbracchio, M. P.; Burnstock, G. Purinergic signaling: Pathophysiological roles. *Jpn. J. Pharmacol.* **1998**, *78*, 113−145. (d) Fischer, B. Therapeutic applications of ATP−(P2)-receptors agonists and antagonists. *Exp. Opin. Ther. Patents* **1999**, *9*, 385−399.

(2) Burnstock, G.; King, B. F. Numbering of cloned P2 purinoceptors. *Drug Dev. Res.* **1996**, *38*, 67−71.

(3) (a) Erb, L.; Garrad, R.; Wang, Y. J.; Quinn, T.; Turner, J. T.; Weisman, G. A. Site-directed mutagenesis of P2U purinoceptors − positively charged amino acids in transmembrane helix-6 and helix-7 affect agonist potency and specificity. *J. Biol. Chem.* **1995**, *270*, 4185−4188. (b) Jiang, Q.; Guo, D.; Lee, B. X.; van Rhee, A. M.; Kim, Y. C.; Nicholas, R. A.; Schachter, J. B.; Harden, T. K.; Jacobson, K. A. A mutational analysis of residues essential for ligand recognition at the human P2Y1 receptor. *Mol. Pharmacol.* **1997**, *52*, 499−507.

(4) (a) Van Rhee, A. M.; Fischer, B.; van Galen, P. J. M.; Jacobson, K. A. Modelling the P2Y purinoceptor using rhodopsin as template. *Drug Des. Discovery* **1995**, *13*, 133−154. (b) Moro, S.; Guo, D.; Camaioni, E.; Boyer, J. L.; Harden, T. K.; Jacobsen, K. A. Human P2Y1 receptor: Molecular modeling and site-directed mutagenesis as tools to identify agonist and antagonist recognition sites. *J. Med. Chem.* **1998**, *41*, 1456−1466. (c) Siddiqi, S. M.; Shaver, S. R.; Pendergast, W.; et al. Molecular modeling of the P2Y2 purinoceptor and synthesis of selected ligands. *Drug Dev. Res.* **1998**, *43*, 33.

(5) (a) Fischer, B.; Boyer, J. L.; Hoyle, C. H. V.; Ziganshin, A. V.; Brizzolara, A. L.; Knight, G. E.; Zimmet, J.; Burnstock, G.; Harden, T. K.; Jacobson, K. A. Identification of potent, selective P2Y-purinoceptor agonists: structure−activity relationships for 2-thioether derivatives of adenosine 5′-triphosphate. *J. Med. Chem.* **1993**, *36*, 3937−3946. (b) Burnstock, G.; Fischer, B.; Hoyle, C. H. V.; Maillard, M.; Ziganshin, A. U.; Brizzolara, A. L.; von Isakovics, A.; Boyer, J. L.; Harden, T. K.; Jacobson, K. A. Structure activity relationship for derivatives of adenosine 5′-triphosphate as agonists at P2-purinoceptors: heterogeneity within P2X and P2Y subtypes. *Drug Dev. Res.* **1994**, *31*, 206−219. (c) Boyer, J. L.; O'Tuel, J. W.; Fischer, B.; Jacobson, K. A.; Harden, T. K. 2-thioether derivatives of adenine nucleotides are exceptionally potent agonists at adenylyl cyclase-linked P2Y-purinoceptors. *Br. J. Pharmacol.* **1995**, *116*, 2611−2616. (d) Zimmet, J.; Järlebark, L.; Hammarberg, T.; van Galen, P. J. M.; Jacobson, K. A.; Heilbronn, E. Synthesis and biological activity of novel 2-thio derivatives of ATP. *Nucleosides Nucleotides* **1993**, *12*, 1−20.

(6) Fischer, B.; Yefidoff, R.; Major, D. T.; Rutman-Halili, I.; Shneyvays, V.; Zinman, T.; Jacobson, K. A.; Shainberg A. Characterization of 'mini-nucleotides' as P2X-receptor agonists in rat cardiomyocyte cultures. An integrated synthetic, biochemical and theoretical study. *J. Med. Chem.* **1999**, *42*, 2685−2696.

(7) (a) Scott, S. P.; Tanaka, J. C. Molecular interactions of 3′,5′-cyclic purine analogues with the binding site of retinal rod iod channels. *Biochemistry* **1995**, *34*, 2338−2347. (b) Brown, R. L.; Bert, R. J.; Evans, F. E.; Karpen, J. W. Activation of retinal rod cGMP-gated channels: what makes for an effective 8-substituted derivative of cGMP? *Biochemistry* **1993**, *32*, 10089−10095.

(8) Halbfinger, E.; Major, D. T.; Ritzmann, M.; Ubl, J. J.; Reiser, G.; Boyer, J. L.; Harden, K. T.; Fischer, B. Molecular recognition of modified adenine nucleotides by the P2Y$_1$-receptor. 1. A synthetic, biochemical, and NMR approach. *J. Med. Chem.* **1999**, *42*, 5325−5337.

(9) Dewar, M. J. S.; Zoebisch, E. G.; Healy, E. F.; Stewart, J. J. P. AM1: A new general purpose quantum mechanical molecular model. *J. Am. Chem. Soc.* **1985**, *107*, 3902−3909.

(10) (a) Hall, G. G. The molecular orbital theory of chemical valency VIII. A method for calculating ionisation potentials. *Proc. R. Soc. London* **1951**, *A205*, 541−552. (b) Roothaan, C. C. J. New developments in molecular orbital theory. *Rev. Mod. Phys.* **1951**, *23*, 69−89.

(11) (a) Ditchfield, R.; Hehre, W. J.; Pople, J. A. Self-consistent molecular orbital methods. IX. An extended Gaussian-type basis for molecular orbital studies of organic molecules. *J. Chem. Phys.* **1971**, *54*, 724−728. (b) Hehre, W. J.; Ditchfield, R.; Pople, J. A. Self-consistent molecular orbital methods. XII. Further extensions of Gaussian type basis sets for use in molecular orbital studies of organic molecules. *J. Chem. Phys.* **1972**, *56*, 2257−2261. (c) Hariharan, P. C.; Pople, J. A. Accuracy of AHn equilibrium geometries by single determinant molecular orbital theory. *Mol. Phys.* **1974**, *27*, 209−214. (d) Gordon, M. S. The isomers of silacyclopropane. *Chem. Phys. Lett.* **1980**, *76*, 163−168. (e) Hariharan, P. C.; Pople, J. A. The influence of polarization functions on molecular orbital hydrogenation energies. *Theor. Chem. Acta* **1973**, *28*, 213−222. (f) Francl, M. M.; Pietro, W. J.; Hehre, W. J.; Binkley, J. S.; Gordon, M. S.; DeFrees, D. J.; Pople, J. A. Self-consistent molecular orbital methods. XXIII. A polarization-type basis set for second row elements. *J. Chem. Phys.* **1982**, *77*, 3654−3665. (g) Frisch, M. J.; Pople, J. A.; Binkley, J. S. Self-consistent molecular orbital methods. 25. Supplementary functions for Gaussian basis sets. *J. Chem. Phys.* **1984**, *80*, 3265−3269.

(12) (a) Krishnan, R.; Binkley, J. S.; Seeger, R.; Pople, J. A. Self-consistent molecular orbital methods. XX. A basis set for correlated wave functions. *J. Chem. Phys.* **1980**, *72*, 650-654. (b) McLean, A. D.; Chandler, G. S. Contracted Gaussian basis set for molecular calculations. I. Second row atoms, Z=11−18. *J. Chem. Phys.* **1980**, *72*, 5639−5648. (c) McGrath, M. P.; Radom, L. Extension of Gaussian-1 (G1) theory to bromine-containing molecules. *J. Chem. Phys.* **1991**, *94*, 511−516. (d) Clark, T.; Chandrasekhar, J.; Spitznagel, G. W.; Schleyer, P. v. R. Efficient diffuse function-augment basis set for anion calculations. III. The 3-21+G basis set for first-row elements, Li−F. *J. Comput. Chem.* **1983**, *4*, 294−301.

(13) (a) Becke, A. D. Density-functional exchange-energy approximation with correct asymptotic behavior. *Phys. Rev. A* **1988**, *38*, 3098−3100. (b) Becke, A. D. Density-functional thermo-

chemistry. III. The role of exact exchange. *J. Chem. Phys.* **1993**, *98*, 5648−5652. (c) Lee, C.; Yang, W.; Parr, R. G. Development of the Colle-Salvetti correlation-energy formula into a functional of the electron density. *Phys. Rev. B* **1988**, *37*, 785−789.

(14) Miertus, S.; Scrocco, E.; Tomasi, J. Electrostatic interaction of a solute with a continuum. A direct utilization of ab initio molecular potentials for the prevision of solvent effects. *Chem. Phys.* **1981**, *55*, 117−129.

(15) (a) Bachs, M.; Luque, F. J.; Orozco, M. Optimization of solute cavities and van der Waals parameters in ab initio MST-SCRF calculations of neutral molecules. *J. Comput. Chem.* **1994**, *15*, 446−454. (b) Cossi, M.; Barone, V.; Cammi, R.; Tomasi, J. Ab initio study of solvated molecules: a new implementation of the polarizable continuum model. *Chem. Phys. Lett.* **1996**, *255*, 327−335.

(16) (a) Cramer, C. J.; Truhlar, D. G. An SCF solvation model for the hydrophobic effect and absolute free energies of aqueous solvation. *Science* **1992**, *256*, 213−217. (b) Cramer, C. J.; Truhlar, D. G. AM1-SM2 and PM3-SM3 parametrized SCF solvation models for free energies in aqueous solution. *J. Comput.-Aided Mol. Des.* **1992**, *6*, 629−666.

(17) (a) Hernández, B.; Orozco, M.; Luque, F. J. Tautomerism of xanthine and alloxanthine: A model for substrate recognition by xanthine oxidase. *J. Comput.-Aided Mol. Des.* **1996**, *10*, 535−544. (b) Hernández, B.; Orozco, M.; Luque, F. J. Role of tautomerism of 2-azaadenine and 2-azahypoxanthine in substrate recognition by xanthine oxidase. *J. Comput.-Aided Mol. Des.* **1997**, *11*, 153−162. (c) Colominas, C.; Luque, F. J.; Orozco, M. Tautomerism and protonation of guanine and cytosine. Implications in the formation of hydrogen-bonded complexes. *J. Am. Chem. Soc.* **1996**, *118*, 6811−6821.

(18) Náray-Szabó, G.; Ferenczy, G. G. Chemical Electrostatics. *Chem. Rev.* **1995**, *95*, 829−847.

(19) Kahn, S. D.; Pau, C. F.; Hehre, W. J. Models for chemical reactivity: Mapping of intermolecular potentials onto electron density surfaces. *Int. J. Quantum Chem., Chem. Symp.* **1988**, *22*, 575−591.

(20) Murray, J. S.; Brinck, T.; Edward Grice, M.; Politzer, P. Correlations between molecular electrostatic potentials and some experimentally based indices of reactivity. *J. Mol. Struct. (THEOCHEM)* **1992**, *256*, 29−45.

(21) Frisch, M. J.; Trucks, G. W.; Schlegel, H. B.; Gill, P. M. W.; Johnson, B. G.; Robb, M. A.; Cheeseman, J. R.; Keith, T. A.; Peterson, G. A.; Montgomery, J. A.; Raghavachari, K.; Al-Laham, M. A.; Zakrzewski, V. G.; Ortiz, J. V.; Foresman, J. B.; Cioslowski, J.; Stefanov, B. B.; Nanayakkara, A.; Challacombe, M.; Peng, C. Y.; Ayala, P. Y.; Chen, W.; Wong, M. W.; Andres, J. L.; Replogle, E. S.; Gomperts, R.; Martin, R. L.; Fox, D. J.; Binkley, J. S.; Defrees, D. J.; Baker, J.; Stewart, J. J. P.; Head-Gordon, M.; Gonzales, C.; Pople, J. A. GAUSSIAN 94 (Rev. C), GAUSSIAN 98 (Rev. A.6); GAUSSIAN Inc.: Pittsburgh, PA, 1995, 1998.

(22) PC Spartan 1.0, Wavefunction, Inc., Irvine, CA.

(23) (a) Ceasar, G. P.; Greene, J. J. Amino-imino tautomerism in the antibiotic formycin A as studied by CNDO/2 molecular orbital theory. *J. Med. Chem.* **1974**, *17*, 1122−1124. (b) Orozco, M.; Lluis, C.; Mallol, J.; Canela, E. I.; Franco, R. Theoretical approximation to the reaction mechanism of adenosine deaminase. *Quant. Struct.-Act. Relat.* **1989**, *8*, 109−114. (c) Orozco, M.; Luque, F. J. Theoretical study of the tautomerism and protonation of 7-aminopyrazolopyrimidine in the gas phase and in aqueous solution. *J. Am. Chem. Soc.* **1995**, *117*, 1378−1386. (d) Orozco, M.; Colominas, C.; Luque, F. J. Theoretical determination of the solvation free energy in water and chloroform of the nucleic acid basis. *Chem. Phys.* **1996**, *209*, 19−29. (e) Hotokka, M.; Lønnberg, H. Hydrolysis of adenosine. A semiempirical and ab initio study. *J. Mol. Struct. (THEOCHEM)* **1996**, *363*, 191−201.

(24) Cramer, C. J.; Truhlar, D. G. Polarization of the nucleic acid bases in aqueous solution. *Chem. Phys. Lett.* **1992**, *198*, 74−80.

(25) Broo, A.; Holmén, A. Ab initio MP2 and DFT calculations of geometry and solution tautomerism of purine and some purine derivatives. *Chem. Phys.* **1996**, *211*, 147−161.

(26) (a) Stewart, R. F.; Jensen, L. H. *J. Chem. Phys.* **1964**, *40*, 2071. (b) Kistenmacher, T. J.; Rossi, M. A refinement of the crystal structure of 9-Methyladenine. *Acta Crystallogr.* **1977**, *B33*, 253−256. (c) Brown, R. D.; Godfrey, P. D.; McNaughton, D.; Pierlot, A. P. A study of the major gas−phase tautomer of adenine by microwave spectroscopy. *Chem. Phys. Lett.* **1989**, *156*, 61−63.

(27) (a) Leszczynski, J. Are the amino groups in the nucleic acid bases coplanar with the molecular rings? Ab initio HF/6-31G* and MP2/6-31G* studies. *Int. J. Quantum Chem., Quantum Biol. Symp.* **1992**, *19*, 43−55. (b) Stewart, E. L.; Foley, C. K.; Allinger, N. L.; Bowen, J. P. Ab initio calculations with electron correlation (MP2) on the nucleic acid basis and their methyl derivatives. *J. Am. Chem. Soc.* **1994**, *116*, 7282−7286. (c) Šponer, J.; Hobza, P. Nonplanar geometries of DNA bases. Ab initio second-order Møller−Plesset study. *J. Phys. Chem.* **1994**, *98*, 3161−3164. (d) Bakalarski, G.; Grochowski, P.; Kwiatkowski, J. S.; Lesyng, B.; Leszczynski, J. Molecular and electrostatic properties of the *N*-methylated nucleic acid bases by density functional theory. *Chem. Phys.* **1996**, *204*, 301−311.

(28) (a) McMullan, R. K.; Benci, P.; Craven, B. M. The neutron crystal structure of 9-Methyladenine at 126 K. *Acta Crystallogr.* **1980**, *B36*, 1424−1430. (b) Craven, B. M.; Benci, P. The charge density and hydrogen bonding in 9-Methyladenine at 126 K. *Acta Crystallogr.* **1981**, *B37*, 1584−1591.

(29) Holmén, A.; Broo, A. A theoretical investigation of the solution N(7)H↔N(9)H tautomerism of adenine. *Int. J. Quantum Chem., Quantum Biol. Symp.* **1995**, *22*, 113−122.

(30) (a) DeVoe, H.; Tinoco, I., Jr. The stability of helical polynucleotides: Base contributions. *J. Mol. Biol.* **1962**, *4*, 500−517. (b) Bergmann, E. D.; Weiler-Feilchenfeld, H.; Neiman, Z. An experimental investigation of the tautomers of adenine. *J. Chem. Soc.* **1970**, *B*, 1334−1336.

(31) The experimental dipole moment values of 9-Me-A and 9-benzyl-A were found to be 3.25 and 2.75 D in dioxane, respectively, by Bergman et al. (ref 30b). However, solvent effects might have been present, as dioxane has been reported to give discrepancies of several tenths of debye (ref 30b). DeVoe et al. (ref 30a) found the dipole moment of 9-*n*-butyl-A to be 3.0 D in CCl4, and this has been an accepted approximate value for the dipole moment of adenine (ref 33a,b and 34a). Thus, it might be more appropriate to use 3.0 D as the reference value for the dipole moment value of 9-Me-A and adenine in the gas phase, rather than 3.25 D.

(32) (a) Wolfenden, R. V. Tautomeric equilibria in inosine and adenosine. *J. Mol. Biol.* **1969**, *40*, 307−310. (b) Zamora, F.; Kunsman, M.; Sabat, M.; Lippert, B. Metal-stabilized rare tautomers of nucleobases. 6. Imino tautomer of adenine in a mixed-nucleobase complex of mercury(II). *Inorg. Chem.* **1997**, *36*, 1583−1587.

(33) (a) Pullman, B.; Berthod, H.; Dreyfus, M. Relatio amine-imine tautomerism in adenines. *Theor. Chim. Acta (Berlin)* **1969**, *15*, 265−268. (b) Norinder, U. A theoretical reinvestigation of the nucleic bases adenine, guanine, cytosine, thymine and uracil using AM1. *J. Mol. Struct. (THEOCHEM)* **1987**, *151*, 259−269. (c) Katritzky, A. R.; Karelson, M. AM1 calculations of reaction field effects on the tautomeric equilibria of nucleic acid pyrimidine and purine bases and their 1-Methyl analogues. *J. Am. Chem. Soc.* **1991**, *113*, 1561−1566.

(34) Mely, B.; Pullman, A. Ab initio calculations on cytosine, thymine and adenine. *Theor. Chim. Acta (Berlin)* **1969**, *13*, 278−287.

(35) Orozco, M.; Hernández, B.; Luque, F. J. Tautomerism of 1-methyl derivatives of uracil, thymine, and 5-bromouracil. Is tautomerism the basis for the mutagenicity of 5-bromouridine? *J. Phys. Chem. B.* **1998**, *102*, 5228−5233.

(36) (a) Bonnaccorsi, R.; Scrocco, E.; Tomasi, J.; Pullman, A. Ab initio molecular electrostatic potentials. Guanine compared to adenine. *Theor. Chim. Acta* **1975**, *36*, 339−344. (b) Alkorta, I.; Perez, J. J. Molecular polarization potential maps of the nucleic acid bases. *Int. J. Quantum Chem.* **1996**, *57*, 123−135.

(37) (a) Platts, J. A.; Howard, S. T.; Bracke, B. R. F. Directionality of hydrogen bonds to sulfur and oxygen. *J. Am. Chem. Soc.* **1996**, *118*, 2726−2733. (b) Salai Cheettu Ammal, S.; Venuvanalingam, P. Ab initio and DFT investigations of lithium/hydrogen bonded complexes of trimethylamine, dimethyl ether and dimethyl sulfide. *J. Chem. Soc., Faraday Trans.* **1998**, *94*, 2669−2674.

(38) (a) Saenger, W. *Principles of Nucleic Acid Structure*; Springer-Verlag: New York, 1984; pp 107−110; (b) p 21.

(39) (a) Russo, N.; Toscano, M.; Grand, A.; Jolibois, F. Protonation of thymine, cytosine, adenine, and guanine DNA nucleic acid bases: Theoretical investigation into the framework of density functional theory. *J. Comput. Chem.* **1998**, *19*, 989−1000. (b) Smets, J.; Houben, L.; Schoone, K.; Maes, G.; Adamowicz, L. Multiple site proton affinities of methylated nucleic acid bases. *Chem. Phys. Lett.* **1996**, *262*, 789−796.

(40) Kim, K.; Friesner, R. A. Hydrogen bonding between amino acid backbone and side chain analogues: A high level ab initio study. *J. Am. Chem. Soc.* **1997**, *119*, 12952−12961.

JM9901576